

Chernogolovka 2000: Mesoscopic and strongly correlated electron systems

6. Quantum computing

Macroscopic quantum superposition of current states in a Josephson-junction loop

F K Wilhelm, C H van der Wal, A C J ter Haar,
R N Schouten, C J P M Harmans, J E Mooij,
T P Orlando, S Lloyd

Abstract. Superconducting circuits with Josephson tunnel junctions are interesting systems for research on quantum-mechanical behavior of macroscopic degrees of freedom. A particular realization is a small superconducting loop containing three Josephson junctions. Close to magnetic frustration $1/2$, the physics of this system corresponds to a double well, whose minima correspond to persistent currents of opposite sign. We present DC measurements of the flux indicating a smooth transition close to the degeneracy point even at very low temperatures. Furthermore, microwave-spectroscopy experiments allow for the excitation to the next excited state. The dependence of the energy of the resonance on the applied flux clearly indicates the nature of these states as tunneling-splitted superpositions of flux states. We theoretically analyze the system using a generalized master-equation formulation of the spin-boson model. We address the nature of the measuring process by a switching DC SQUID and the possible interpretation of the spectroscopy data in terms of quantum coherence. We discuss these aspects in the context of further applications as a quantum bit.

1. Introduction: qubits and MQC

Since the formulation of quantum mechanics, its concepts have been heavily disputed. They can now be directly verified in the microscopic world of systems with very few degrees of freedom such as NMR, ion traps, or cavity QED. With present-day technology, such microscopic systems can be controlled externally. This has led to the proposal of a quantum computer, which makes explicit use of the possibility to create superpositions and allows to solve certain computational problems with a qualitatively reduced number of steps (see [1] for a recent review). The

aforementioned quantum systems have been used to demonstrate few-bit quantum computation, however, it appears to be very difficult if at all possible to integrate them into larger circuits.

Solid state electronics, on the other hand, can be very easily integrated. Moreover, in the field of mesoscopic physics, and in particular in mesoscopic superconductivity, genuine quantum-mechanical phenomena have already been demonstrated. This makes mesoscopic superconductors a candidate for the realization of quantum computation [2–5]. More specifically, we propose to utilize persistent-current states of small superconducting loops containing at least three Josephson junctions [4]. These states correspond to the collective motion of all superconducting electrons in the loop, hence they are macroscopic [6].

In this contribution, we are going to briefly outline the idea of our device [4] and present experimental results tracing the ground state as well as results of microwave spectroscopy [7]. The data show clear evidence of anti-crossing of energy levels, hence proving that around degeneracy, the system's eigenstates are superpositions of the two basis current states. The results will be further discussed in terms of macroscopic quantum superpositions and coherence. By creating a superposition of these states, which is necessary for quantum computation, we also address a fundamental issue in quantum mechanics: a Schrödinger's cat state. We acknowledge that the mere superposition does not exclude alternative theories for quantum mechanics (e.g. macrorealistic theories [8]). This would require a type of experiment as proposed by Leggett et al. [9].

2. The device

A single small Josephson tunnel junction with a capacitance C and a coupling energy E_J can be represented as a particle of mass C in a periodic potential, where the phase ϕ represents the coordinate, and the number of Cooper pairs is the conjugate momentum. Our system (Fig. 1a), consists of a micrometer-sized loop of negligible geometric inductance penetrated by a magnetic flux Φ_{ext} close to half a

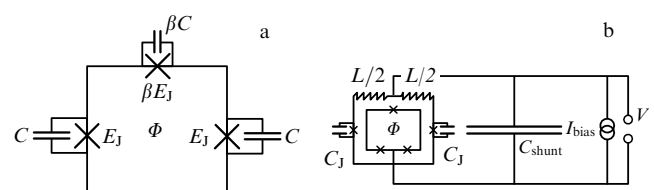


Figure 1. Schematic drawing of the qubit (a) and the measuring circuit (b). Crosses indicate Josephson junctions.

F K Wilhelm, C H van der Wal, A C J ter Haar, R N Schouten,
C J P M Harmans, J E Mooij Department of Applied Physics and
DIMES, Delft University of Technology, Lorentzweg 1, 2628 CJ Delft,
The Netherlands

J E Mooij, T P Orlando Department of Electrical Engineering and
Computer Science, Massachusetts Institute of Technology, Cambridge
MA, USA

S Lloyd Department of Mechanical Engineering, Massachusetts Institute
of Technology, Cambridge MA, USA

superconducting flux quantum Φ_0 . The loop contains three such junctions, whose phases are locked together by the applied flux due to the phase quantization condition, hence leading to a two-dimensional coordinate space. It has been demonstrated [4, 5], that by proper choice of the junction parameters, this effective potential is a periodic pattern of local double wells, whose minimums correspond to clock- and counter-clockwise supercurrent, respectively. The double wells are separated by strong potential barriers such that they are mutually very well uncoupled, whereas the barrier within a double well is sufficiently weak such that it can be overcome by quantum tunneling. The energy of the two minima can be controlled by tuning the applied external flux away from $\Phi_0/2$. The system parameters can be chosen such that there is only one bound state in each well. This renders the low-temperature (less than 100 mK) physics of the system equivalent to a two-level system. It has been predicted [10], that the intrinsic sources of noise and decoherence (quasi-particles, nuclear spins ...) allow for quantum-coherent behavior up to a decoherence time of $\tau_\phi = 1$ ms.

This setup invokes some key ideas of the ‘conventional’ MQC-proposal using an RF-SQUID [9, 11], with the key difference that no self-inductance is needed in order to form the double-well potential. This allows for much smaller loop sizes and hence facilitates the decoupling from environmental noise. Nevertheless, results similar to ours have recently been obtained in an RF-SQUID [12]. Other observations that have been related to macroscopic superposition states are tunnel splittings observed with magnetic molecular clusters [13] and quantum interference of C_{60} molecules [14]. In quantum dots [15] and superconducting circuits where charge effects dominate over the Josephson effect [16, 17] superpositions of charge states as well as quantum-coherent charge oscillations [18] have been observed.

The state of the qubit can be read out by a DC-SQUID magnetometer which detects the flux produced by the circulating current. Due to the small inductance of the system, this signal is only a small fraction of Φ_0 . Moreover, according to first principles of quantum mechanics, any measuring device (or ‘meter’) tends to decohere the quantum state. As we expect the quantum coherence to be very fragile, this property deserves special attention. In order to ensure sufficient coherence we have to guarantee that (i) the meter does not decohere the system while not measuring and (ii) the meter registers the result before the relaxation time, i.e. after the macroscopic environment constituted by the meter has put the qubit into a thermal mixture of states, wiping out the signatures of the initial state.

This decoherence is realized through the coupling to the external impedance. The measuring SQUID has two macroscopic phase degrees of freedom, which we choose as follows: one is associated with the circulating current in the SQUID’s loop (internal degree of freedom), the other is associated with the bias current through the SQUID (external degree of freedom). As the bias current is ramped up, the coupling between these two degrees of freedom increases strongly, due to the nonlinearity of the SQUID’s current-phase relations [19]. The external variable is coupled to a dissipative environment. The internal degree of freedom has negligible intrinsic damping and the associated mass (i.e. the capacitance of the junctions of the SQUID) is very small. This means that the circulating current is non-dissipative and does not disturb the system, i.e. there is little dephasing as long as we do not apply a measuring current.

In order to further minimize the unwanted decoherence in our device, we use a setup which uses only very few dissipative elements: an undamped SQUID with unshunted junctions with low critical current and no extra resistors. In order to still reduce fluctuations of the SQUID, it was made ‘heavy’ by shunting with a large superconducting capacitor.

This SQUID has a highly hysteretic $I-V$ characteristic [19]. The flux is determined through the switching current which provides a measure for the effective Josephson coupling across the SQUID. The escape to a voltage state is a stochastic process, which leads to a wide spread of those switching currents (see, e.g. [20] for an overview). The width of the switching current histogram in our experiments corresponds to a standard deviation in the flux readout of $11 \times 10^{-3} \Phi_0$, so the uncertainty in flux readout is much larger than the flux signal from the qubit $2MI_p \approx 3 \times 10^{-3} \Phi_0$. This width is much bigger than expected from simple theoretical models [20]. This may be due to quantum fluctuations of the circulating current (and consequently the total flux through the SQUID) and is subject of enduring investigation. In order to obtain the results presented in this paper, substantial statistical averaging over repeated measurements was necessary in order to get sufficient resolution. Consequently only ensemble-averaged quantities can be measured.

3. Experiments

The system was realized by microfabricating a micrometer-sized aluminum loop with unshunted Josephson junctions, using the technology described in Ref. [21]. Around the loop we fabricated the DC-SQUID magnetometer (Fig. 1b), with smaller Josephson junctions that were as underdamped as the junctions of the inner loop. Loop parameters estimated from test junctions fabricated on the same chip and electron-microscope inspection of the measured device give a critical current amplitude $I_{C0} = 570 \pm 60$ nA and $C = 2.6 \pm 0.4$ fF for the largest junctions in the loop. The size of the small junction is reduced by a factor $\beta = 0.82 \pm 0.1$, giving $E_J/E_{Ch} = 38 \pm 8$ and a circulating current in one of the potential minima of $I_p = 450 \pm 50$ nA. These parameters allow for a tunnel matrix element t/h between 0.2 and 5 GHz. The parameters of the DC-SQUID junctions were $I_{C0} = 109 \pm 5$ nA and $C_S = 0.6 \pm 0.1$ fF. The self-inductance of the inner loop and the DC-SQUID loop were estimated to be 11 ± 1 pH and 16 ± 1 pH respectively, and the mutual inductance M between the loop and the SQUID was 7 ± 1 pH.

4. Ground state measurements

In a first series of experiments, we have detected the flux produced by the qubit as a function of the static bias flux. We compare it to the expectation value for a quantum-mechanical two-level system coupled to a bath at temperature T ,

$$\langle \Phi_q \rangle = \Phi_a \frac{\epsilon}{\Delta E} \tanh\left(\frac{\Delta E}{2k_B T}\right), \quad (1)$$

where Φ_a is the flux produced when the system is purely in one of the classical states, $\Delta E = (\epsilon^2 + 4t_{\text{eff}}^2)^{1/2}$ is the energy splitting of the quantum-mechanical levels and $\epsilon = \epsilon(\Phi_{\text{ext}}) \propto \Phi - \Phi_0/2$ is the energy difference of the classical states. In general, this function shows a step around $\epsilon = 0$, which is

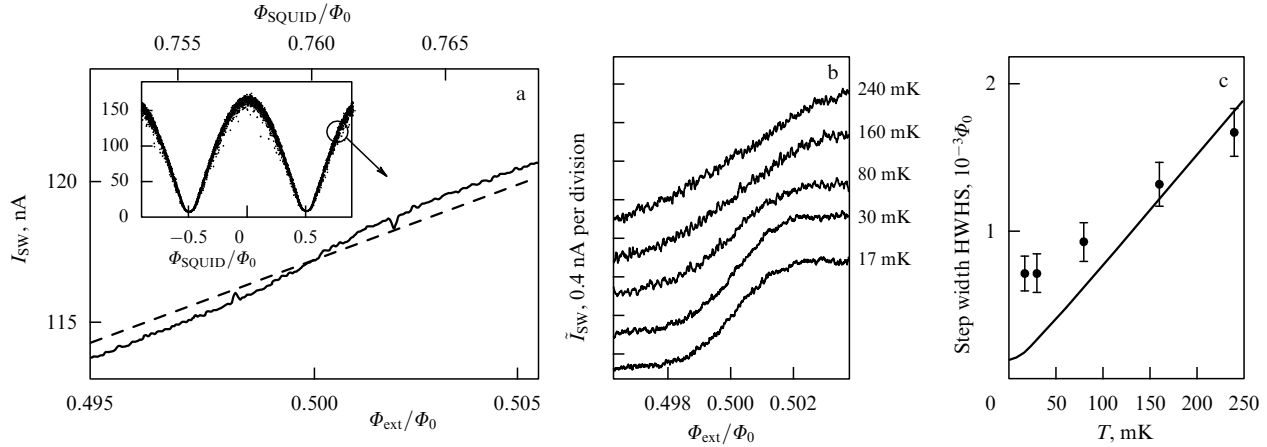


Figure 2. Switching-current levels of the DC-SQUID versus applied flux. (a) The main figure shows the averaged level of I_{SW} (solid line) near $\Phi_{ext} \approx \Phi_0/2$ which happens to be $\Phi_{SQUID} = 0.76 \Phi_0$ and the rounded step at $\Phi_{ext} = \Phi_0/2$ indicates the change of sign in the persistent current. The spikes are due to additionally applied microwaves. The inset shows the modulation of I_{SW} versus the flux Φ_{SQUID} applied to the DC-SQUID loop (data not averaged, one point per switching event). (b) Measured qubit flux from the qubit for different temperatures. The background signal resulting from flux directly applied to the SQUID-loop is subtracted. (c) Analysis of the step width (half-width at half-step, HWHS). The solid line corresponds to the extrapolation of equation (1), assuming the spectroscopically measured t_{eff} .

rounded due to thermal and quantum fluctuations. As $T \rightarrow 0$, the system is in its ground state and quantum fluctuations dominate. Any residual rounding is controlled by a finite tunneling matrix element t_{eff} and indicates that the ground state close to the degeneracy point is a superposition.

Experimentally, the step occurs on top of the bias flux through the SQUID (see Fig. 2a). The step width decreases with temperature (see Fig. 2b) but stays finite. The observed step width is even much broader than expected from quantum rounding on the scale of the value of t that was found with spectroscopy (see Fig. 2c). The width saturates at an effective temperature of about 100 mK. The high effective temperature of the loop can be the result of heating induced by the DC-SQUID after the switching. As the qubit is well isolated from the environment, this heat only relaxes very slowly.

5. Spectroscopy

On top of the DC-flux, which fixes the energy bias ϵ of our two-level system, we periodically modulate ϵ using continuous microwaves. Figure 3a shows the flux signal of the inner loop. On top of the step described in the previous section, each trace shows a peak and a dip symmetrically around $\Phi_{ext} = \Phi_0/2$, which were absent when no microwaves were applied. The positions of the peaks and dips in Φ_{ext} depend on microwave frequency f but not on amplitude. They reflect microwave-induced transitions to the state with a persistent current of opposite sign, they occur when the microwave frequency is resonant with the energy splitting $\Delta E = hf$. As the frequency is lowered, the resonances are moving towards the center, Fig. 3a.

In Figure 3b half the distance in Φ_{ext} between the resonant peak and dip is plotted for all frequencies f , which represents $\Delta E(\epsilon)$. The relation between ΔE and Φ_{ext} is linear at high frequencies. The slope of this part translates into $I_p = 484 \pm 2$ nA, in good agreement with the predicted value. At lower frequencies the energy splitting levels off, hence indicating a finite tunnel splitting of $t_{eff}/h \approx 0.33 \pm 0.03$ GHz. The level separation very close to $\Phi_0/2$ could not be measured directly since at this point the

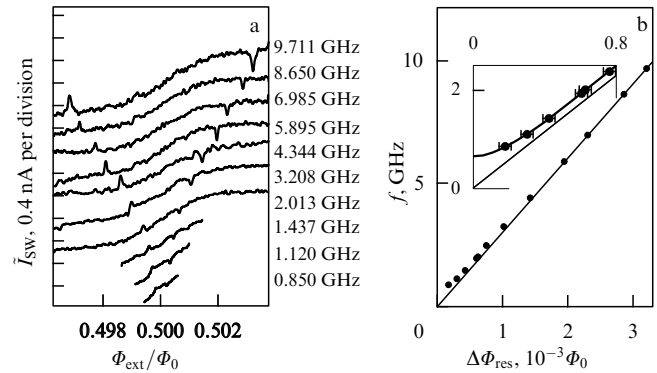


Figure 3. Results of cw-microwave spectroscopy. (a) Traces at fixed frequency showing resonances corresponding to pumping to the respective excited state. Symmetrically around $\Phi_0/2$ the signal shows a peak and a dip, which are only observed with measurements in the presence of the microwaves. They are due to resonant transitions between the loop's two quantum levels (see Fig. 2). Different curves represent different values of Φ_{ext} , measured at different microwave frequencies f (labels on the right). (b) Resonance positions are a clear indication of an anti-crossing. Half the distance in Φ_{ext} between the resonant peak and dip $\Delta\Phi_{res}$ at different microwave frequencies f (f is plotted on the vertical axis). Peak and dip positions are determined from traces as in Fig. 2a. At high frequencies the $\Delta\Phi_{res}$ values are proportional to the microwave frequency. The inset: the thin line is a linear fit through the high frequency data points and zero. The thick line is a fit of the energy eigenvalues with only the tunnel coupling t as a fitting parameter, yielding $t_{eff}/h = 0.33 \pm 0.03$ GHz.

expectation value for the persistent current is zero for both the ground state and the excited state. The measured value of t is compatible with the predicted value of t . As the predicted value depends exponentially on sample parameters and hence has a substantial uncertainty, a quantitative analysis of a possible suppression of t_{eff} due to a bosonic [22] or spin-bath [23] environment is not possible. The fact that we see a finite tunnel splitting indicates that the damping of our quantum system by environmental degrees of freedom is weak. The dimensionless dissipation parameter α [22] must be $\alpha < 1$.

This level repulsion close to the degeneracy point clearly indicates that the eigenstates, between which the transitions

occur, are superpositions of the localized basis states. At $\Phi_{\text{ext}} = \Phi_0/2$, these are symmetric and antisymmetric superpositions of the two classical persistent-current states which have respectively lower and higher energies than the localized classical states.

6. Nonlinear regime

In Figure 4a we show the dip at a fixed frequency of 5.895 GHz for different microwave amplitudes. The dip amplitude and the full width at half the maximum amplitude (FWHM) were extracted by fitting a Lorentzian peak shape to the data. Figure 4b shows that the dip amplitude increases rapidly for microwave amplitudes up to $V_{\text{AC}} \approx 2$ a. u., followed by a saturation for larger microwave amplitudes. The saturated dip amplitude is ≈ 0.25 nA, which is close to half the full step height of the rounded step at $\Phi_0/2$ (≈ 0.4 nA) in Fig. 2b. This indicates that on resonance the energy levels are close to being equally populated, as expected for continuous pumping.

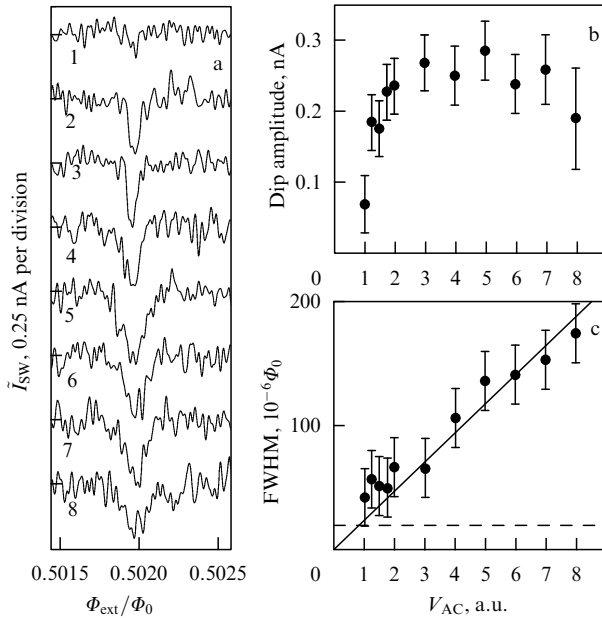


Figure 4. Results of cw-microwave spectroscopy at fixed frequency but different power. (a) The influence of the microwave amplitude on the shape of the resonance dip in the scaled switching current I_{SW} , measured at 5.895 GHz (the labels on the left give the amplitude V_{AC} in a.u.). (b) Resonance amplitude first increases with microwave amplitude V_{AC} , but saturates at $V_{\text{AC}} > 2$ a.u. (c) Resonance width as a function of the microwave power. The full-width-half-maximum (FWHM) of the dips increases with V_{AC} . The linear fit through the highest data points and zero is a guide to the eye. The horizontal dashed line is at a flux value that corresponds to the shift in effective flux bias Φ_{ext} that is induced when the bias current is ramped through the DC-SQUID. This acts as a flux instability with an amplitude of $\approx 20 \times 10^{-6}\Phi_0$. Resonance lines with a FWHM below this value cannot be observed.

Figure 4c shows a linear dependence between the FWHM and the microwave amplitude, as we would expect it for the Rabi resonance of a strongly and coherently driven two-level system [24]: the linear dependence of the FWHM on microwave amplitude in Fig. 4c suggests that the linewidth is indeed dominated by the frequency of microwave-induced Rabi transitions. In the presence of weak decoherence, the

Rabi oscillations decay over a time T_2 into a stationary mixture of ‘eigenstates’ of the driven system known as Floquet states. After T_2 , transitions between those states only occur due to incoherent processes. Even in this case, the peaks remain narrow Lorentzians [25, 26] which depend on the external parameters analogously to Rabi peaks: the FWHM of the Lorentzian resonance line is proportional to the amplitude of the monochromatic driving [24]. This allows to observe narrow resonances even after T_2 . Using the linear relation between ΔE and Φ_{ext} for Φ_{ext} values away from $\Phi_0/2$, the observed FWHM in Φ_{ext} units can be expressed in frequency units. This indicates a Rabi frequency of, for example, 150 MHz at $V_{\text{AC}} = 4$ a.u.

The loss of dip amplitude and the apparent saturation of the FWHM at low V_{AC} is either caused by variations in the flux bias Φ_{ext} (corresponding to inhomogeneous broadening for the ensemble average [27]) or by an intrinsic dephasing mechanism. The effective dephasing time T_2^* [27] can be deduced from the FWHM at low V_{AC} . The FWHM (expressed in energy units) of a resonance-line shape that is dominated by a finite dephasing time corresponds to $2\hbar/T_2^*$ [24, 27]. From our data, we find $T_2^* \approx 5$ ns, which allows for a few Rabi cycles. This is another hint on the presence of coherent Rabi dynamics, however, only time-resolved measurements would be fully conclusive. Possible sources for the relatively short value of T_2^* will be discussed in the following Section.

7. Discussion

The DC-SQUID performs a measurement on a single quantum system. As described above, our setup in principle still allows for reasonable dephasing and mixing times. The external electronics limits the ramping speed, so the SQUID is coupled to the qubit longer than theoretically required and is consequently strongly dephasing the qubit prior to the actual measurement. This can be avoided in future experiments by the use of more efficient measuring schemes.

The loss of dip amplitude in Fig. 4 is probably not due to the noise, but due to a small deterministic contribution to the effective Φ_{ext} from the circulating current in the DC-SQUID. The SQUID is operated at $0.76\Phi_0$ in its loop, where its circulating current depends on the bias current due to its nonlinear behavior [19], so the readout happens at a bias flux slightly altered due the SQUID. This bias flux depends on the switching current level, which in turn has a broad spread due to the large histograms described in the beginning of this paper. This means that data recorded by switching events for low bias side of I_{bias} differ in flux bias on the inner loop from that of the high current levels by $20 \times 10^{-6}\Phi_0$. Resonance lines at low V_{AC} (i. e. with a FWHM $< 20 \times 10^{-6}\Phi_0$) cannot be observed as the peaks and dips smear out when averaging over many switching events. The loss of dip amplitude and the apparent saturation of the FWHM at low V_{AC} is probably dominated by this mechanism for inhomogeneous line broadening and *not* by dephasing.

8. Concluding remarks and future prospects

We show clear experimental evidence of level repulsion in a small superconducting loop containing three Josephson junctions, which can behave as a macroscopic quantum two-level system. We demonstrate a useful readout for the magnetization of the loop scheme by an underdamped DC-SQUID.

This demonstrates the potential of these loops for further work on macroscopic quantum coherence and solid-state quantum computing. This requires quantum state control with pulsed microwaves and development of measurement schemes that are less invasive. Multiple qubit circuits with controlled coupling are within reach using present-day technology.

We thank J B Majer, A C Wallast, L Tian, D S Crankshaw, J Schmidt, A Wallraff, L S Levitov, M Grifoni, and D Esteve for help and stimulating discussions. This work was financially supported by the Dutch Foundation for Fundamental Research on Matter (FOM), the European TMR Research Network on Superconducting Nanocircuits (SUPNAN), the USA Army Research Office (Grant DAAG55-98-1-0369) and the NEDO Joint Research Program (NTDP-98).

References

1. Bennet C H, DiVincenzo D *Nature* **404** 247 (2000)
2. Makhlin Yu, Schön G, Shnirman A *Nature* **398** 305 (1999)
3. Ioffe L B et al. *Nature* **398** 679 (1999)
4. Mooij J E et al. *Science* **285** 1036 (1999)
5. Orlando T P et al. *Phys. Rev. B* **60** 15398 (1999)
6. Anderson P W, in *Lectures on the Many-Body Problem* Vol. 2 (Ed. E R Caianiello) (New York: Academic Press, 1964) p. 113; Leggett A J *Prog. Theor. Phys. Suppl.* **69** 80 (1980); Likharev K K *Usp. Fiz. Nauk* **139** 169 (1983) [*Sov. Phys. Usp.* **26** 87 (1983)]
7. Van der Wal C H et al. *Science* **290** 773 (2000)
8. For an in-depth discussion on macrorealism see the essays of Leggett A J, Shimony A, in *Quantum Measurement: Beyond Paradox* (Eds R A Healey, G Hellman) (Minneapolis: Univ. Minnesota Press, 1998) p. 1
9. Leggett A J, Garg A *Phys. Rev. Lett.* **54** 857 (1985)
10. Tian L et al., in *Quantum Mesoscopic Phenomena and Mesoscopic Devices in Microelectronics* (Dordrecht: Kluwer, 2000) p. 429
11. Leggett A J *J. Supercond.* **12** 683 (1999)
12. Friedman J R et al. *Nature* **406** 43 (2000)
13. Wernsdorfer W, Sessoli R *Science* **284** 133 (1999)
14. Arndt M et al. *Nature* **401** 680 (1999)
15. Oosterkamp T H et al. *Nature* **395** 873 (1998)
16. Nakamura Y, Chen C D, Tsai J S *Phys. Rev. Lett.* **79** 2328 (1997)
17. Bouchiat V et al. *Phys. Scripta T* **76** 165 (1998)
18. Nakamura Y, Pashkin Yu A, Tsai J S *Nature* **398** 786 (1999)
19. Tinkham M *Introduction to Superconductivity* (New York: McGraw-Hill, 1996)
20. Martinis J M, Devoret M H, Clarke J *Phys. Rev. B* **35** 4682 (1987)
21. Van der Wal C H, Mooij J E *J. Supercond.* **12** 807 (1999)
22. Leggett A J et al. *Rev. Mod. Phys.* **59** 1 (1987)
23. Prokof'ev N, Stamp P *Rep. Prog. Phys.* **63** 669 (2000); cond-mat/0001080
24. Cohen-Tannoudji C, Diu B, Laloë F *Quantum Mechanics* Vol. 1 (New York: Wiley, 1977) p. 443
25. Wilhelm F K, Grifoni M (in preparation)
26. Grifoni M, Hänggi P *Phys. Rep.* **304** 229 (1998)
27. Abragam A *Principles of Nuclear Magnetism* (Oxford: Oxford Univ. Press, 1961) p. 39

Quantum Andreev interferometer in an environment

Y M Gal'perin, L Y Gorelik, N I Lundin, V S Shumeiko, R I Shekhter, M Jonson

Abstract. The influence of a noisy environment on coherent transport in Andreev states through a point contact between two superconductors is considered. The amount of dephasing is estimated for a microwave-activated quantum interferometer. Possibilities of experimentally investigating the coupling between a superconducting quantum point contact and its electromagnetic environment are discussed.

1. Introduction

The assumption of coherent transport in Andreev states in a superconducting quantum point contact (SQPC) is widely used in theoretical work, see, e.g., the items of Ref. [1]. However, in realistic systems, interactions with a dynamical environment will always introduce some amount of dephasing, see the items of Ref. [2] for a review.

The so-called microwave-activated quantum interferometer (MAQI) [3] is a device proposed as a tool to study the dynamics of Andreev levels (ALs), present in a superconducting point contact. It is based on a short, single-mode, weakly biased SQPC which is subject to microwave irradiation. Confined to the contact area there are current-carrying Andreev states. The corresponding energy levels — Andreev levels — are found in pairs within the superconductor energy gap Δ , one below and one above the Fermi level. If an SQPC is short ($L \ll \xi_0$ where L is the length of the junction while ξ_0 is the superconductor coherence length), there is only one pair of Andreev levels and their positions depend on the order parameter phase difference, ϕ , across the contact as

$$E_{\pm} = \pm E(\phi) = \pm \Delta \sqrt{1 - D \sin^2\left(\frac{\phi}{2}\right)}. \quad (1)$$

The two states carry current in opposite directions and in equilibrium at low temperature only the lower state is populated. The applied bias, V , through the Josephson relation $\dot{\phi} = 2eV/\hbar$, forces the Andreev levels to move adiabatically within the energy gap with a period of $T_p = \hbar\pi/eV$, see Fig. 1.

The microwave field induces Landau – Zener (LZ) transitions between the Andreev levels (indicated by wavy lines in Fig. 1). If the upper level is populated after the second transition, a delocalized quasi-particle excitation will be created when this Andreev level merges with the continuum. The result will be a dc contribution to the current. Further, this current exhibits an interference pattern since there are two paths with different phase gains available to the upper

Y M Gal'perin University of Oslo, P. O. Box 1048 Blindern, N-0316 Oslo Norway

A F Ioffe Institute of the Russian Academy of Sciences, 194021 St. Petersburg, Russian Federation

L Y Gorelik, N I Lundin, V S Shumeiko, R I Shekhter, M Jonson Chalmers University of Technology, Department of Applied Physics, and Göteborg University, 412 96 Göteborg, Sweden